

Press Forming Analysis Contributing to the Expansion of High Strength Steel Sheet Applications[†]

ISHIWATARI Akinobu *¹ URABE Masaki *² INAZUMI Toru *³

Abstract:

JFE Steel has developed new technologies in order to predict stretch flange fracture and to reduce springback for applying high tensile strength steel sheet to more diverse automobile parts. The technology which uses maximum principal strain gradient was developed to predict stretch flange fracture. By this technology, the accurate prediction of stretch flange fracture, which cannot be predicted by forming limit diagram, was obtained. The factor analysis technology of springback was developed to reduce springback in high strength steel press parts. The analysis specifies the area of parts which affects most on springback. By using the analysis, it became possible to obtain the effective solution to reduce the springback.

1. Introduction

In recent years, improved automobile fuel economy has been demanded from the viewpoint of reducing CO₂ and other environmental load substances, and in response, efforts are being made to reduce auto body weight. Higher auto body strength has also been demanded with the aim of further improving crashworthiness. Although makers have expanded the application of high tensile strength steel to structural parts in order to address these problems¹⁾, prevention of fracture during press forming, particularly at blank edges, and securing dimensional accuracy have become important issues for greater use of high strength steel sheets²⁾.

In forming of high tensile strength steel, the forming

mode has changed from drawing to crush-forming, and as a result, fractures from the blank edge, which cannot be predicted accurately by fracture analysis with the forming limit diagrams (FLD) used until now, have become a frequent occurrence. This type of fracture occurs during stretch-forming of flange parts, such as flange-up forming, bore expanding (burring), etc. and is called stretch flange fracture. To enable computer prediction of this type of fracture, JFE Steel developed a stretch flange fracture prediction technology³⁾ using the maximum principal strain gradient and applied this technology to computer aided engineering (CAE) analysis.

In securing dimensional accuracy of high tensile strength steel parts, identification of the factors which cause springback and establishment of appropriate countermeasures is effective. Therefore, JFE Steel developed a factor analysis technique for springback by controlling stress at the press bottom dead point position⁴⁾.

2. Stretch Flange Fracture Prediction Technology

The forming limit diagrams and other techniques are generally used in fracture prediction in CAE analysis of press forming of steel sheets. However, as prediction of the deformation limit of the flange edge in flange-up forming and bore expanding (burring) involves a different fracture mechanism from the deformation limit of the sheet interior, prediction as actual phenomena is not possible by using FLD.

As factors which influence the deformation limit in stretch flange deformation, mechanical properties⁵⁾, the

[†] Originally published in *JFE GIHO* No. 30 (Aug. 2012), p. 19–24



*¹ Senior Researcher Manager,
Forming Technology Res. Dept.,
Steel Res. Lab.,
JFE Steel



*² Dr. Eng.,
Senior Researcher Manager,
Forming Technology Res. Dept.,
Steel Res. Lab.,
JFE Steel



*³ Dr. Eng.,
General Manager, Forming Technology Res. Dept.,
Steel Res. Lab.,
JFE Steel

forming conditions of the sheared edge^{6,7)}, and the maximum principal strain gradient⁸⁾ may be mentioned. Among these, the influence of mechanical properties and the forming conditions of the sheared edge have been studied quantitatively, but virtually no quantitative studies have been carried out in connection with the maximum principal strain gradient. Therefore, several types of bore expanding tests were performed with different maximum principal strain gradients using various types of steel sheets. As results, the influence of the maximum principal strain gradient on the stretch flange deformation limit was clarified quantitatively³⁾, and a technology for prediction of stretch flange fracture by CAE analysis was developed.

2.1 Influence of Maximum Principal Strain Gradient on Critical Strain for Stretch Flange Limit

The strain gradients which are considered to influence the stretch flange limit are thought to comprise two types. One type, which is termed the strain gradient in the radial direction, is the gradient of the maximum principal strain (circumferential strain) in the direction at right angles to the maximum principal strain (radial direction) in a punched hole. The second type, called the strain gradient in the circumferential direction, is the gradient of the maximum principal strain in the direction of the maximum principal strain (circumferential direction). This section describes the results of an investigation of the effects of these strain gradients on the maximum principal strain at the fracture limit, i.e., the critical strain for fracture.

2.1.1 Experimental conditions

As test materials, 5 grades of steel sheets from mild steel to 980 MPa class high tensile strength steel were prepared, as shown in **Table 1**. First, the test conditions for studying the influence of the radial strain gradient on the critical strain for stretch flange fracture are shown in **Table 2**. Bore-expanding tests were performed using 3 levels of initial hole diameter (10 mm, 25 mm, 50 mm)

Table 1 Thickness and mechanical properties of examined steels

Steel	Thickness (mm)	YS (MPa)	TS (MPa)	El (%)	λ (%)
A	1.2	168	309	49	155
B	1.2	330	459	35	107
C	1.2	419	643	28	62
D	1.2	603	823	20	72
E	1.2	787	1 005	18	47

YS: Yield strength TS: Tensile strength El: Elongation
 λ : Hole expansion limit with conical punch

Table 2 Experimental conditions to investigate the influence of strain gradient in the radial direction

Initial hole diameter in blank (mm)	Punch shape	Applied steel
10	60°conical	A, B, C, D, E
25		A, B, C, D, E
50		A, B, C, D, E
10	ϕ 50 mm cylindrical	A, B, C
25	ϕ 80 mm cylindrical	A, B, C
	ϕ 50 mm cylindrical	D, E
50	ϕ 150 mm cylindrical	A, B, C
	ϕ 100 mm cylindrical	D, E

Table 3 Experimental conditions to investigate the influence of strain gradient in circumferential direction

Steel	Initial hole shape		Clearance (%)	Initial hole diameter in blank (mm)
	Semi major axis (mm)	Semi minor axis (mm)		
C	50	10	12.5	80
	50	30		

in the punch blank, and 2 punch shapes (60° conical and flat-bottomed cylindrical), for a total of 6 combinations of punch conditions.

It may be noted that the punch clearance relative to the sheet thickness was constant at 12.5% in all cases, and during the flat-bottomed cylindrical bore-expanding test, the punch diameter was changed appropriately, corresponding to the material properties, so that the fracture position was at the hole edge. The test conditions for studying the influence of the strain gradient in the circumferential direction on the critical strain for stretch flange fracture are shown in **Table 3**. Here, the strain gradient in the circumferential direction was changed by performing the flat-bottomed cylindrical bore-expanding test with an elliptical initial hole shape.

2.1.2 Effect of initial hole diameter on hole expansion limit

The effect of the initial hole diameter of the blank on the hole expansion limit when using a conical punch is shown in **Fig. 1**. When the initial hole diameter is d_0 and the fracture diameter is d , the hole expansion limit λ is expressed as follows:

$$\lambda = (d - d_0) / d_0 \times 100 (\%) \dots\dots\dots (1)$$

As can be understood from Fig. 1, the hole expansion limit decreases as the initial hole diameter increases. In other words, it is difficult to use the hole expansion limit provided in the material specification without modifica-

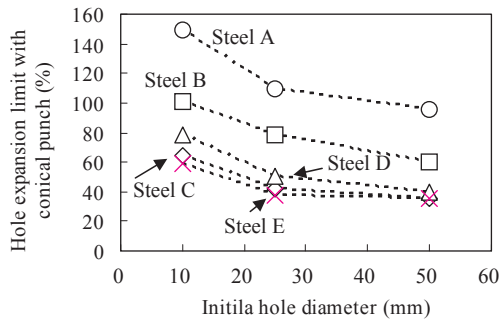


Fig. 1 Effect of initial hole diameter in blank on hole expansion limit with conical punch

tion in actual pressing, where the initial hole diameter changes diversely. Thus, the development of a prediction method using a new index is considered necessary.

2.1.3 Effect of maximum principal strain gradient in radial direction on critical strain for fracture

The effect of the maximum principal strain gradient in the radial direction on the critical strain for fracture of the hole edge is shown in Fig. 2. The critical strain for fracture was calculated from the hole expansion limit

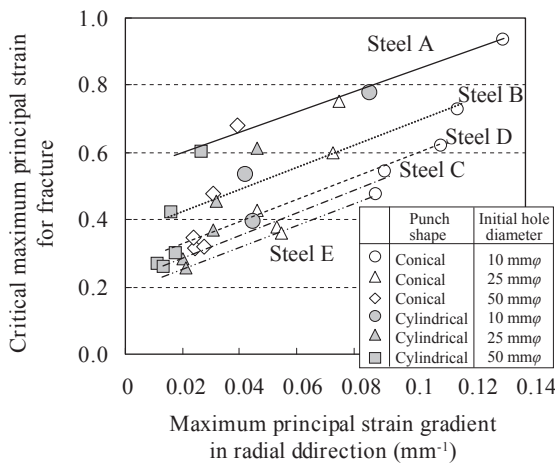


Fig. 2 Effect of the maximum principal strain gradient in the radial direction on critical strain for fracture

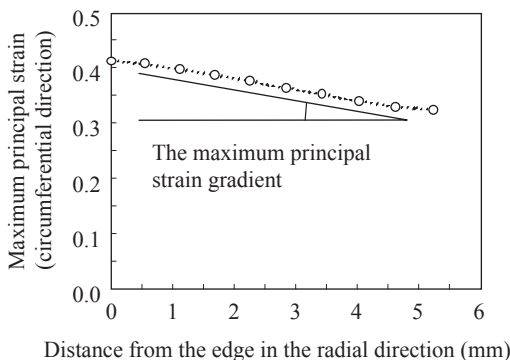


Fig. 3 Gradient of maximum principal strain

assuming constant strain at the hole edge. The maximum principal strain gradient in the radial direction is shown schematically in Fig. 3. The maximum principal strain gradient in the radial direction is defined as the average gradient of the maximum principal strain over a radial distance of 5 mm from the hole edge in the fractured hole diameter, and is calculated by CAE. The software used in CAE was LS-DYNA ver. 971 produced by Livermore Software Technology. As a result, it was understood that the critical strain for fracture in stretch-flange edge increases in a substantially linear manner accompanying increases in the maximum principal strain gradient in the radial direction with all materials, and is independent of the punch shape. This is explained by the fact that, when the maximum principal strain gradient in the radial direction becomes large, the suppression of strain localization effect and the necking growth suppression effect^{8,9)} in the region where strain is small increase because the interior does not reach a condition of strain localization under uniaxial tension, even though that condition is achieved at the hole edge.

Based on the study outlined above, the fracture limit can be arranged by the maximum principal strain gradient in the radial direction and the maximum principal strain at the hole edge, independent of forming conditions such as the initial hole diameter, the shape of the hole-expanding punch, etc.

2.1.4 Effect of maximum principal strain gradient in circumferential direction on critical strain for fracture

In actual parts, a gradient sometimes exists in the maximum principal strain direction (circumferential direction), for example, when the hole diameter is not uniform, when the height of flange-up forming varies, etc. Therefore, the effect of the maximum principal strain gradient in the circumferential direction on the critical strain for fracture was studied by performing a

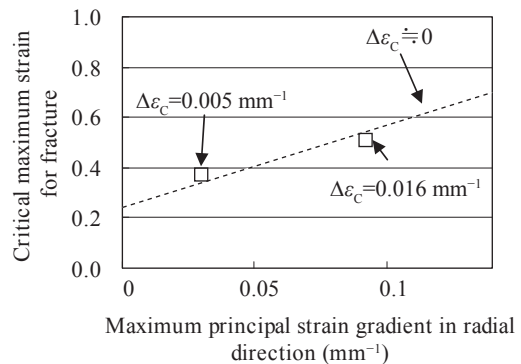


Fig. 4 Effect of maximum strain gradient in the circumferential direction ($\Delta\epsilon_c$) on critical maximum principal strain

flat-bottom cylindrical bore-expanding test in which the punching shape was elliptical. The results are shown in **Fig. 4**. The critical strain line obtained in Fig. 2 for material C is also shown here. The critical strain for fracture and the maximum principal strain gradient in a flat-bottom cylindrical bore-expanding test with an elliptical punching shape were calculated by analysis with finite element method (FEM)^{2,10}.

Based on the fact that the critical strain for fracture in the case where a maximum principal strain gradient exists in the circumferential direction, and critical strain line obtained from Fig. 2, where the maximum principal strain gradient is considered to be substantially 0, are on virtually the same level, the effect of the maximum principal strain gradient in the circumferential direction on the critical strain for fracture is considered to be extremely small. This is thought to be because the suppression of strain localization effect and the necking growth suppression effect are predominantly acting toward the crack propagation direction.

2.2 Application to CAE Forming Analysis

The experimental results in the previous section demonstrated that it is possible to predict stretch flange fracture using the maximum principal strain gradient in the radial direction and the critical strain for fracture. This section describes the results when this prediction method was incorporated in general-purpose CAE analysis, and an analysis was performed with part shapes.

2.2.1 Results of press forming

The shape of a laboratory press part simulating the center pillar lower, which was used in the experiments and calculations, is shown in **Photo 1**. For press-forming experiments, two types of steel sheets with a thickness of 1.2 mm and the properties shown in **Table 4** were prepared. Material F is a material with a λ value, as pro-



Photo 1 Pressed part

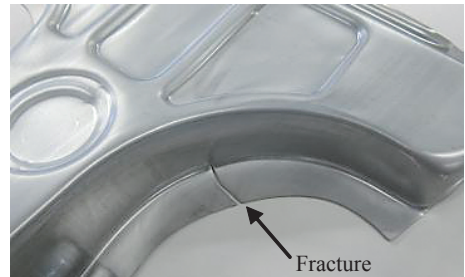
Table 4 Mechanical properties of steel used in press forming

Material	YS (MPa)	TS (MPa)	El (%)	λ (%)
F	437	624	34.1	92
G	398	640	32.3	68

YS: Yield strength TS: Tensile strength El: Elongation
 λ : Hole expansion limit with conical punch



(a) Material F



(b) Material G

Photo 2 Results of press forming

vided in the Japan Iron and Steel Federation Standard¹¹), which is 20% or more larger than that of material G. Photographs of the press-formed stretch flange parts are shown in **Photo 2**. Cracking did not occur in material F, but did occur in material G.

2.2.2 Results of press-forming analysis

A CAE analysis of this press-forming experiment was performed. **Figure 5** shows the results of an FLD evaluation, which is performed in general fracture prediction. It can be understood that accurate stretch flange fracture prediction was not possible with this conventional method, as the FLD method predicted no cracking in both material F and material G.

The strain (maximum principal strain) at the flange edge at the part where fracture occurred in the press-forming experiment and the maximum principal strain gradient at the perpendicular direction were predicted by FEM. The results for material F were maximum principal strain, 0.31 and maximum principal strain gradient, 0.003 2, whereas the corresponding results for material G were 0.33 and 0.003 2, respectively. These results were plotted together with the critical strain line for stretch flange fracture, which was obtained separately, as

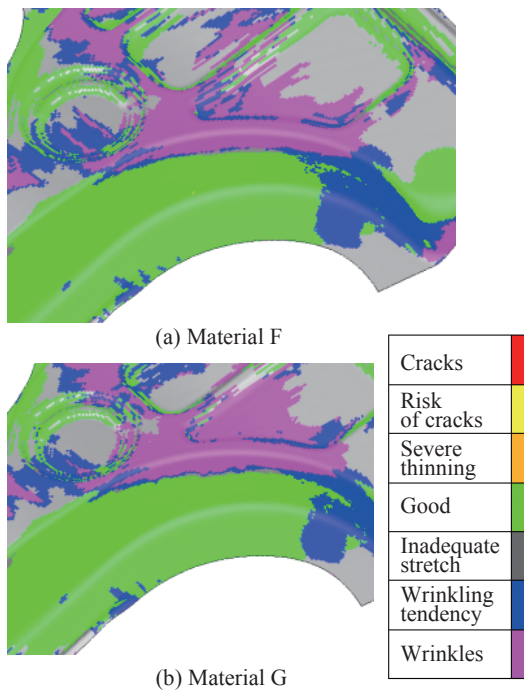


Fig. 5 Pressed part

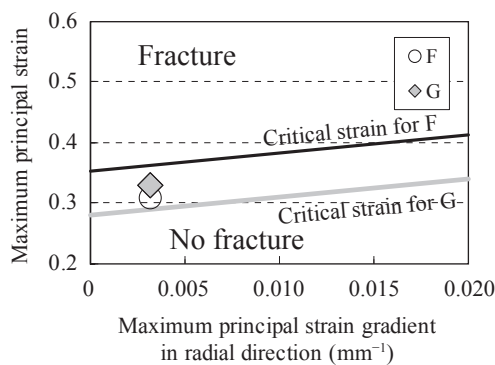


Fig. 6 Evaluation of stretch flange fracture by maximum principal strain in radial direction and strain gradient

shown in Fig. 6. Since the plot for material F is below the critical strain line for stretch flange fracture, it can be predicted that fracture will not occur. In contrast, the plot for material G lies above the critical strain line for fracture, and fracture was predicted. These CAE results are in agreement with the condition of fracture in the experimental results, showing that the stretch flange fracture prediction method using the maximum principal strain gradient is also valid for actual parts.

3. Springback Factor Analysis Technique

The springback which occurs in press-forming of high tensile strength steel is extremely large, and becomes a problem in automobile body accuracy and the auto assembly process.

Therefore, it is important to form high tensile strength steel to the target dimensions. Since an early date, springback countermeasures were adopted by the

allowance of the die, shape modification of the excess metal, and so on. It was difficult to implement effective countermeasures for springback, since by small changes in die geometry dramatic improvements in springback were realized in some cases, while there were also cases in which there was virtually no change in springback. Therefore, a factor analysis method for springback⁴⁾ was developed, which makes it possible to predict the positions in parts where springback countermeasures, etc. can be applied effectively by CAE analysis.

3.1 Procedure of Factor Analysis of Springback

The procedure of factor analysis of springback is shown in the flow chart in Fig. 7. First, an FEM analysis of forming is performed, and the stress distribution of the pressing bottom dead point (center) is obtained. Next, the stress in a certain part is eliminated, and a springback analysis is performed using that stress distribution. The effect of the stress at that part on springback is obtained by performing a shape comparison with the results of conventional springback analysis.

3.2 Example of Factor Analysis of Springback

The example of the curved hat shown in Fig. 8 is discussed here as an example of factor analysis of springback. The cross section of the hat is 45 mm × 45 mm, its length is approximately 500 mm, and its angle of curvature is 135°. Press-forming was performed by draw-forming using a blank holding pressure of 700 kN.

The mechanical properties of the blank material used in this study are shown in Table 5. The sheet thickness is 1.2 mm.

In this study, the object of analysis was torsion generated in forming of the curved hat. In these torsion measurements, the torsional angles at the right and left ends were evaluated when the center of the curved part was fixed as shown in Fig. 8. First, as shown in Fig. 9, a springback analysis was performed by broadly dividing the curved hat into the flange areas (F1, F2) web area

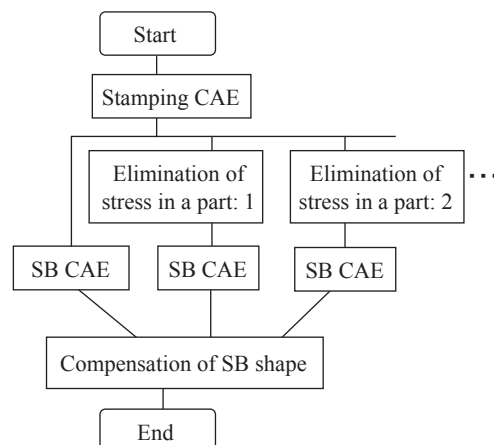


Fig. 7 Flow chart of factor analysis of springback (SB)

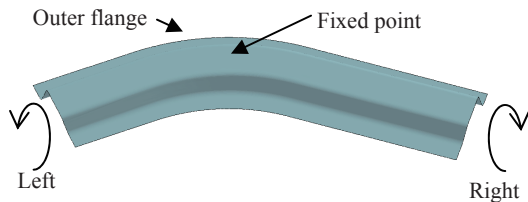


Fig. 8 Curved hat and fixed point in torsion measurement

Table 5 Mechanical properties of 590 MPa grade steel used for the factor analysis technology of spring back (SB)

Material	YS (MPa)	TS (MPa)	E1 (%)	\bar{r}
590R	484	625	26.7	1.0

YS: Yield strength TS: Tensile strength El: Elongation
 \bar{r} : Lankford value

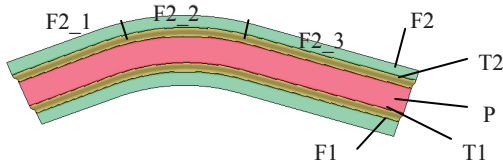


Fig. 9 Areas where stress eliminated

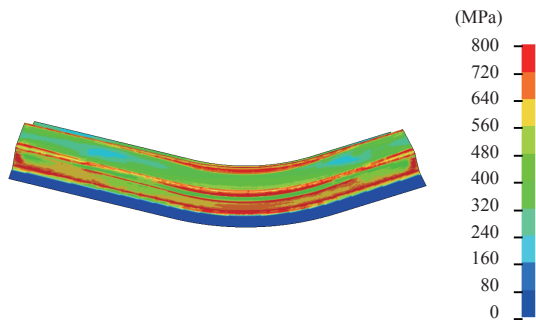


Fig. 10 Equivalent stress distribution in the case of which stress in F2 is eliminated

(P), and wall areas (T1, T2), which include the R area, and eliminating stress in these respective areas. The stress distribution before the springback analysis in which the stress in part F2 on the outer side flange part is shown in Fig. 10. The results of an investigation of the effect of stress elimination from the respective areas on improvement of the torsional angle are shown in Fig. 11. From this, it can be understood that the effect of stress elimination in the outer flange F2 was comparatively large, whereas elimination of stress from the web area had a large negative effect on the torsional angle. In other words, in flange parts and the like, the amount of springback can be reduced by reducing the compression at the pressing bottom dead point, but on the other hand, in the web part, further increase of the tensile stress in this part is necessary in order to reduce torsion.

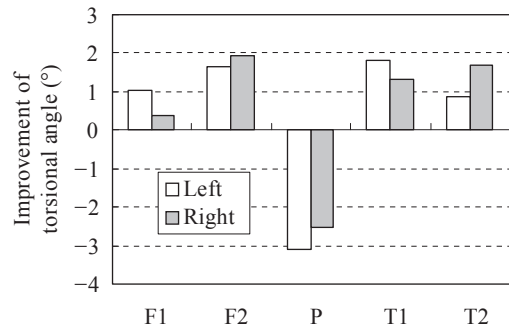


Fig. 11 Effect of stress elimination from each area on improvement of torsional angle

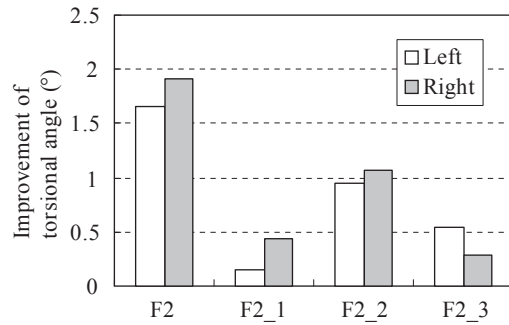


Fig. 12 Effect of stress elimination from each area on improvement of torsional angle in the outer flange part

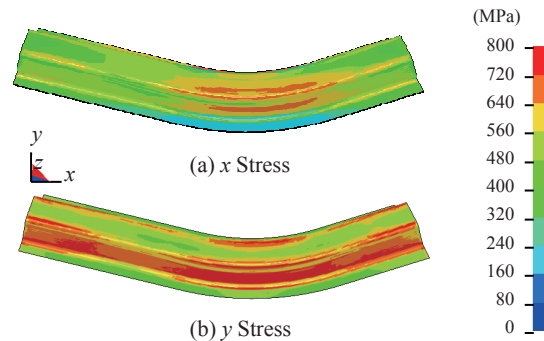


Fig. 13 Stress distribution before stress elimination

Next, an analysis of the outer flange part F2, where the torsion improvement effect was comparatively large, was performed by dividing the F2 area into the curved flange area (F2-2), short straight flange area (F2-1), and long straight flange area (F2-3). The results are shown in Fig. 12.

It can be understood that the torsion improvement effect is large in the curved part. The stress distributions for the x and y directions of this curved flange part are shown in Fig. 13. As a large stress distribution was observed in the x direction of the curved part, it is estimated that this x direction stress distribution has a large effect on improvement of the torsional angle.

Based on the factor analysis of springback described above, it is considered that the curved flange part influ-

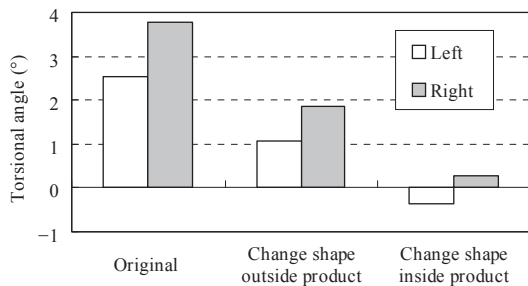


Fig. 14 Improvement by shape change

ences springback, and the springback can be reduced if the stress distribution in this part is reduced. When the stress in the curved part was reduced by reducing and changing the curved part by changing the excess metal part and the product part of the die, a large improvement in the torsional angle was possible, as shown in **Fig. 14**.

4. Conclusion

JFE Steel developed new technologies for stretch flange fracture and poor dimensional accuracy, which have become issues for expanded use of high tensile strength steels.

A technology which enables accurate prediction of stretch flange fracture using the maximum principal strain gradient was developed. This technology makes it possible to predict stretch flange fracture, which could not be predicted with the general FLD used in forming

analysis until now.

A technology for factor analysis of springback was also developed. This technology enables prediction of the parts and stress locations which are the origin of poor dimensional accuracy in high tensile strength steel parts, and thereby makes it possible to establish more effective countermeasures for springback.

References

- 1) Yoshitake, Akihide; Ono, Moriaki; Urabe, Masaki. *Jour. Soc. Automotive Eng. Jpn.* 2005, vol. 59, no. 11, p. 4.
- 2) Urabe, Masaki; Tamai, Yoshikiyo; Yoshitake, Akihide; Toyoda, Daisuke; Sato, Yoshihito. *58th Proc. Jpn. Joint Conf. Tech. Plasticity.* 2007, p. 535–536.
- 3) Iizuka, Eiji; Urabe, Masaki; Yamasaki, Yuji; Inazumi, Toru. *Jour. Jpn. Soc. Tech. Plasticity.* 2010, vol. 51, no. 594, p. 700–705.
- 4) JFE Steel. Urabe, Masaki. *Press seikei kaiseki hoho.* Japanese Patent 4894294.
- 5) Nakagawa, Takeo; Takita, Michio; Yoshida, Kiyota. *Jour. Jpn. Soc. Tech. Plasticity.* 1970, vol. 11, no. 109, p. 142–151.
- 6) Eiji, Iizuka; Takaaki, Hira; Yoshitake, Akihide. *Jour. Jpn. Soc. Tech. Plasticity.* 2005, vol. 46, no. 534, p. 625–629.
- 7) Toyoda, Daisuke; Sato, Yoshihito; Urabe, Masaki; Tamai, Yoshikiyo; Yoshitake, Akihide. *58th Proc. Jpn. Joint Conf. Tech. Plasticity.* 2007, p. 537–538.
- 8) Nakagawa, Takeo. *Jour. Jpn. Soc. Tech. Plasticity.* 1978, vol. 19, no. 206, p. 227–235.
- 9) Goto, Manabu. *Jour. Jpn. Soc. Tech. Plasticity.* 1993, vol. 34, no. 388, p. 454–461.
- 10) Yoshida, Tohru; Hashimoto, Koji; Aga, Hiroaki. *47th Proc. Jpn. Joint Conf. Tech. Plasticity.* 1996, p. 371–372.
- 11) Japan Iron and Steel Federation Standard. *Method of hole expanding test.* JFS T1001-1996.